The Journal of Experimental Biology 206, 989-998

doi:10.1242/jeb.00198

Electroreception in *G. carapo*: detection of changes in waveform of the electrosensory signals

Pedro A. Aguilera and Angel A. Caputi*

Departamento de Neurofisiología Comparada, Instituto de Investigaciones Biológicas Clemente Estable, Unidad Asociada a Facultad de Ciencias, Universidad de la República, Av. Italia 3318, Montevideo, Uruguay

*Author for correspondence (e-mail: angel@iibce.edu.uy)

Accepted 10 December 2002

Summary

Electric fish evaluate the near environment by detecting changes in their self-generated electric organ discharge. To investigate impedance modulation of the self-generated electric field, this field was measured at the electrosensory fovea of *Gymnotus carapo* in the presence and absence of objects. Changes in local fields provoked by resistive objects were predicted by the change in total energy. Objects with capacitive impedance generated large variations in the relative importance of the different waveform components of the electric organ discharge. We tested the hypothesis that fish discriminate changes in waveform as well as increases in total energy using the novelty response, which is a behavioural response consisting of a transient acceleration of EOD frequency that can follow a change in object impedance. For resistive loads, the amplitude of novelty responses was well predicted by the increase in total energy. For complex loads, the amplitude of novelty responses was correlated not only with increases in total energy but also with waveform changes, consisting of reductions in the early slow negative wave and increases in the late sharp negative wave. The total energy and waveform effects appeared to be additive. These results indicate that *G. carapo* discriminates complex impedance based on an evaluation of different waveform parameters.

Key words: electric image, electrosensory, electric fish, *Gymnotus carapo*, feature discrimination.

Introduction

Electric fish explore the near environment by processing sensory signals evoked by their own self-generated electric fields (Lissmann, 1951, 1958; Lissmann and Machin, 1958). These fields are generated by the activation of electric organs (EO), which transform the fish bodies into a distributed electrical source. The field created by the electric organ discharge (EOD) generates a spatio-temporal pattern of current density that stimulates electroreceptors distributed over the skin. This field constitutes the carrier for active electrolocation signals, resulting from its modulation by objects with impedances different from that of water. The difference between the basal pattern of transcutaneous current density and the pattern in the presence of an object constitutes the electrical image of the object on the skin. Behavioral experiments have shown that both African (Mormyriform) and American (Gymnotiform) electric fish can discriminate objects on the basis of their capacitance (Meyer, 1982; von der Emde, 1990, 1999; von der Emde and Ronacher, 1994).

At every point on the fish's skin, the transcutaneous current results from the sum of the basal field in the absence of the object plus the effect of the object, considered as a virtual electric source (Lissmann and Machin, 1958; Sicardi et al., 2000; Budelli and Caputi, 2000). The electromotive force of such an 'object equivalent source' decreases as a function of object distance and as a function of the absolute value of the object impedance. Since impedance is a complex magnitude, frequency of the local field at the site of the object is an additional important parameter determining the electromotive force of the 'object equivalent source'. Thus, the local characteristics of the electrosensory carrier at the site of the object are critical in measuring object impedance, and differences in the organisation of electrogeneration between species must imply differences in their impedance discrimination strategy.

Mormyriform pulse fish from Africa have a short electric organ located in the tail that generates a basal field with the same waveform everywhere. The waveform is biphasic, with an initial head-positive phase followed by a head-negative phase. In these fish, the waveform of the virtual electromotive force generated by an object is independent of the object's position relative to the fish body. The stimuli resulting from different objects located at the same place in the fish's environment are distributed in a two-dimensional domain in which the axes are the peak-to-peak amplitude of EOD-induced current and the ratio between positive and negative phases of this current. Two receptor types, one sensing the peak-to-peak amplitude of the self-generated local electric organ discharge (sLEOD) and the other sensing a waveform-

related parameter, allow the fish to locate the object in the environment and to measure 'perceptual distances' between points in the two-dimensional domain defined by the amplitude and waveform axes (Bell, 1990; von der Emde, 1990, 1993; von der Emde and Ronacher, 1994; von der Emde and Bell, 1994; von der Emde and Bleckmann, 1997).

Although capacitance discrimination is well-demonstrated in gymnotids, a detailed description of the stimulus domain is lacking and the mechanism of capacitance detection in pulse gymnotiforms is not yet understood (von der Emde, 1999). The electric organ of pulse gymnotid fish is quite different from that of pulse mormyriform fish. Pulse gymnotids have a long electric organ that extends along 90% of the fish body. The organ is not homogeneous along its length and it generates complex spatio-temporal fields and waveforms that are highly dependent on its position in the field (Bastian, 1977; Watson and Bastian, 1979; Caputi, 1999; Assad et al., 1999). This suggests that the strategy for impedance discrimination must be quite different in pulse gymnotids from that in pulse mormyriforms.

Wave gymnotids emit a quasi-sinusoidal carrier that is modulated in phase and amplitude by nearby objects. Electroreceptors are well tuned to the main frequency of the EOD and therefore the impedance-related sensory qualities of an electrolocated object could be related to the change in amplitude and phase of the sLEOD (Hopkins, 1983; Dye and Meyer, 1986). In wave gymnotids, amplitude is measured by the P-type electroreceptors and phase is measured by T-type receptors. Scheich et al. (1973) showed in the wave gymnotid *Eigenmannia* sp. that T- and P-types of electroreceptors '*respond differently in such a manner that information is provided to the brain adequate to distinguish capacitive from resistive impedance and to assess the magnitude of the mixture in complex impedance*'. Further support for this argument is provided by the demonstrated neural mechanism in these fish that allows them to discriminate signals in the phase-amplitude domain (cf. Heiligenberg, 1991).

Very little is known about impedance discrimination in pulse gymnotids. The electric organ of these fish generates a complex spatio-temporal electric field resulting from the weighted sum of the effects of a series of electric sources having different time-waveforms and internal resistances (Caputi, 1999; Aguilera et al., 2001). The sensory side of the system is also complex, in that four types of tuberous electroreceptors have been described (Bastian, 1976, 1977; Watson and Bastian, 1979). The complexity of the system has led us to the hypothesis that these fish have the ability to discriminate different features in the reafferent signal waveform and to classify object images in a multidimensional 'perceptual domain'.

This paper describes the changes generated by objects of different impedance on the amplitude and waveform of the self-generated local electric field (sLEOD) of the pulse gymnotid *Gymnotus carapo* (L). There is a zone around the mouth where receptor density is highest and where the variety of receptor types is highest (the electrosensory fovea; Castelló et al., 2000). This anatomo-functional variety is necessary for implementing complex impedance discrimination. Thus, our study is focused on the electrosensory fovea. The paper also examines the changes in reafferent electrosensory input that are able to provoke 'novelty responses' (a well-known orienting behavior, Lissmann; 1958; Bullock, 1969). These behavioural experiments allowed us to test the hypothesis that these fish are able to discriminate two types of stimulus parameters, some correlated with the total energy and others only dependent on waveform.

Materials and methods

Eighteen sexually undifferentiated *Gymnotus carapo* L., 12–25 cm in length, were used in this study. These are South American pulse-emitting, weakly electric fish. The fish were gathered in the Laguna del Sauce, Uruguay, under the regulations of the Ministry of Ganadería y Agricultura. All experiments complied with regulations of the Committee for Use of Experimental Animal of the IIBCE and according to the guidelines of the Society for Neuroscience and the International Guiding Principles for Biomedical Research Involving Animals.

Fish were held within a net in the middle of a tank (18 cm×25 cm×10 cm) containing 3 liters of water with a conductivity of 100 μS cm^{-1}. We used the technique introduced by von der Emde (1990) to modulate the reafference, i.e. the transcutaneous current evoked by the fish's own EOD. A cylindrical 'object' (2 mm diameter, 1 cm length) was oriented with its long axis perpendicular to the skin of the electrosensory fovea (Castelló et al., 2000). The two ends of the cylinder were made of conducting carbon discs that were inserted into a non-conducting plastic tube. The carbon discs were connected to a switch by insulated copper wires leaving the tube at its center. The switch allowed us to apply a capacitive-resistive load (z) between the bases of the stimulus-object. The component of the sLEOD perpendicular to the skin was measured as the voltage drop between the bare tip of a 100 μm diameter insulated copper wire placed against the skin and the base of the stimulus-object cylinder nearest to the fish (see inset in Fig. 1). The voltage drop between the carbon ends of the object was also recorded in most experiments. Signals were amplified (×100) and filtered (band pass 10–10 000 Hz) for observation of individual LEOD waveforms using a digital oscilloscope, and sampled (20 kHz, 12-bit resolution) for off-line processing. To characterise the waveform generated in the presence of a given stimulus-object impedance, we averaged 64 consecutive sLEODs for each load in each fish. We compared time waveforms and their fast Fourier transforms. To compare amplitude and waveform obtained when applying different loads to the object, sLEODs were plotted against the sLEOD obtained in the absence of load impedance. The difference in amplitude was shown by the different inclination of the lines and the differences in waveform by the deviation of the loop from a straight line.

To evaluate if *G. carapo* is able to discriminate between two different local stimuli we used a 'comparative unidimensional judgement' procedure, a psychophysical method in which a

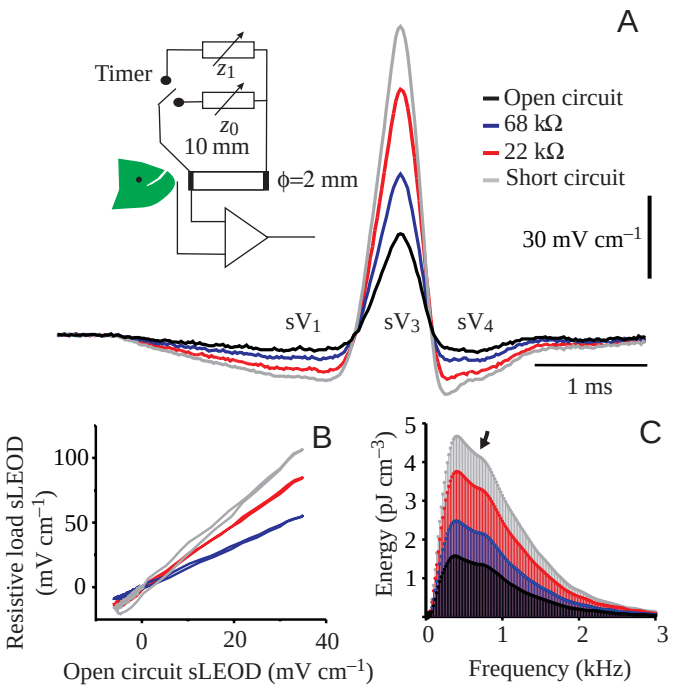

Fig. 1. Modulation of the sLEOD by loading the stimulus-object with resistors. (A) The diagram illustrates the methodology employed. LEOD of *Gymnotus carapo* was recorded between an electrode adjacent to the skin and the closest base of a cylindrical object placed 2 mm away from the skin. The electrode was a 100 µm bare-tip insulated wire; the object consisted of a plastic tube 2 mm diameter (ϕ) and 10 mm long with a carbon plug electrode in each opening. An external variable impedance z_0 was connected to the carbon plugs to modify the object longitudinal impedance. To evaluate impedance discrimination, a second impedance was alternatively connected using a timed switch. Changes in object longitudinal resistance resulted in marked changes in image contrast as shown by recorded sLEOD waveforms corresponding to open circuit (black), 22 kΩ (red), 68 kΩ (blue) and short circuit (gray; same color code throughout the figure). To align the traces we used as a time reference a far-field recording of the EOD that was not modified by the presence of our small stimulus-object. (B) sLEOD corresponding to the three first loads as a function of the sLEOD corresponding to open circuit. Note the small phase shift. (C) Spectral density of the same signals. The ordinate corresponds to the energy dissipated locally during eacy EOD. Note the hump in the high frequency shoulder of all spectra (arrow).

baseline waveform is applied in alternation with a comparison waveform (Werner, 1980). We used an orienting response (the novelty response) as an index of stimulus discrimination. This response, consisting of a transient acceleration of EOD frequency, has been used extensively to test the ability of fish to detect changes in sensory stimuli (Szabo and Fessard, 1965; Bullock, 1969; cf. Hopkins, 1983; Moller, 1995).

In each experiment, an external variable impedance z_0 was connected to the carbon plugs to set the baseline sLEOD. A timed switch was used to substitute z_0 with a second variable impedance z_1 to set the comparison sLEOD (Fig. 1, inset). Each trial consisted of ten cycles of 30 s periods (connecting z_0 for 29 s and z_1 for 1 s). For each trial, the inter-EOD interval was displayed off-line as a function of time to test for the presence of novelty responses. A novelty response was said to occur when duration of the second interval (I_2) after presenting the comparison sLEOD was below the inferior confidence limit of the baseline interval (I_0, defined as the mean of the preceding 5 baseline inter-EOD intervals, confidence limit=I_0–2 S.E.M.) The amplitude of the novelty response was defined as the maximum shortening of the normalised interval [novelty response amplitude = $(1–I_2/I_0)\times100$].

We explored the novelty responses following transitions between: (i) open circuit (z_0) and either a pure resistive or pure capacitive impedance (z_1, 5 fish); (ii) pairs of impedance (z_0 and z_1) causing sLEODs with the same total energy, as measured by their equal root mean square (rms) value (5 fish); (iii) short circuit (z_0) and either a pure resistive or pure capacitive impedance (z_1, 4 fish). In all cases we studied the amplitude of the novelty response provoked by transitions in both directions (z_0 to z_1 and *vice versa*).

Results

Modulation of the sLEOD at the foveal region.

The sLEOD at the electrosensory fovea of *G. carapo* shows three main waveform components: sV$_1$, sV$_3$ and sV$_4$, where the prefix s indicates 'self generated local' and V$_x$ is the EOD generating component (using the nomenclature introduced by Aguilera et al., 2001) (Fig. 1A). A plastic cylinder with conducting carbon discs at both ends was used to explore the effect of longitudinal impedance changes on the sLEOD. When the ends of the cylindrical stimulus-object were not connected (open circuit), the current intensity along the longitudinal axis was null and the sLEOD was minimal (peak-to-peak amplitude was 0.6 of the basal value in the absence of the object). When the ends of the cylindrical stimulus-object were short-circuited, the current flowing along the longitudinal axis and the sLEOD were maximal (approximately 2.5–3 times the value obtained with open circuit). Therefore, maximum and minimum effective values (rms values) of the reafferent signal were caused by short circuit and open circuit, respectively (grey and black labels, Fig. 1). Between these boundaries, the rms value decreased monotonically with object resistance. When time was standardised using the head-to-tail EOD as a reference (Fig. 1B), the corresponding sLEOD values between waveforms obtained using different resistive loads were very well correlated (r^2>0.99), indicating a very similar waveform and a minimum phase shift (Fig. 1B).

The amplitudes of individual wave components were unequivocally determined by a 'one to one' function of the rms value, indicating that a single parameter, tightly correlated with the total energy, is enough to characterise the signal when the object impedance is purely resistive. However, small but systematic changes in waveform were also observed. The relative amplitude of sV$_1$ (sV$_1$/sV$_3$) decreased with object resistance, as did the sharpness and relative amplitude of sV$_4$ (sV$_4$/sV$_3$, Fig. 1A). As expected by the good correlation

between waveforms obtained with different load resistances, the general shapes of the power spectral density histograms were very similar: a sharp increase, a peak (at 350–500 Hz), and a slow decay vanishing within the noise above 3 kHz. The smooth decay of the power at the high frequency flank was interrupted by a hump (at 700–1000 Hz) of constant amplitude when it was normalised to the peak (arrow, Fig. 1C).

For capacitive loads within the range 0.3–300 nF, sLEOD energy (as measured by rms value) amplitude increased as a function of capacitance. Below 0.3 nF the observed sLEODs were similar to those obtained without connecting any load (open circuit) and above 300 nF the recorded sLEODs were similar to those obtained by short-circuiting the object bases

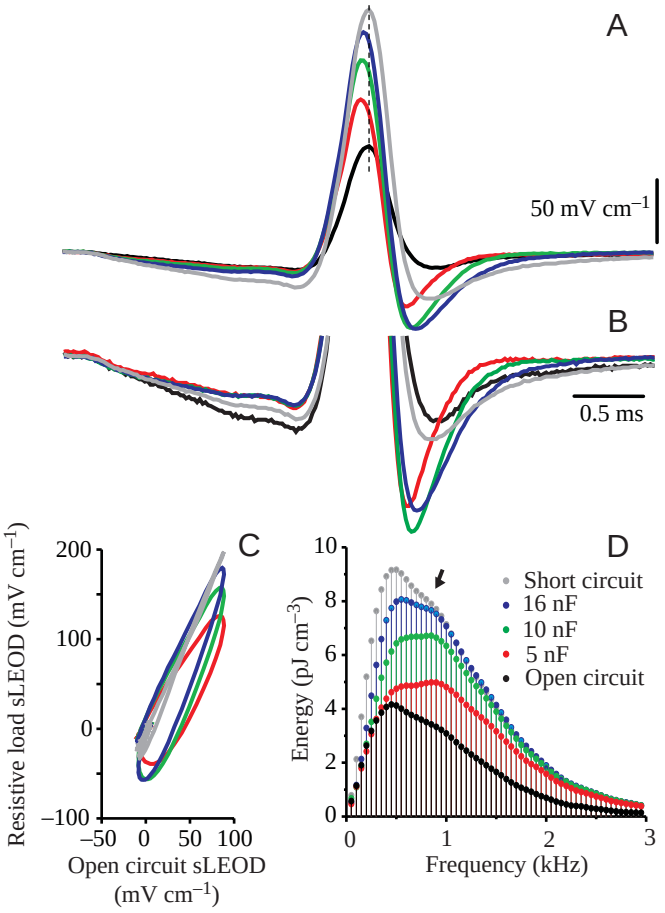

Fig. 2. Modulation of the sLEOD by loading the stimulus-object with capacitors. (A) sLEOD waveforms corresponding to open circuit (black), 16 nF (blue), 10 nF (green), 5 nF (red) and short circuit (grey; same color code throughout the figure). (B) Normalised waveforms (with respect to sV_3) to compare the relative values of sV_1, sV_4 and the phase advance of the slope sV_3–sV_4. (C) sLEOD corresponding to the four first loads as a function of the sLEOD corresponding to open circuit. Note the large phase shift. (D) Spectral density of the same signals. Ordinate corresponds to the energy dissipated locally during each EOD. Note that the relative amplitude of the humps in the high frequency shoulder (arrow) increases for intermediate loads, becoming the absolute maximum for 10 nF and 5 nF (red and green traces, respectively).

(Fig. 2A). Important changes in sLEOD waveform were provoked by capacitive loads, in contrast to the small ones provoked by resistive loads. Mid-range capacitive loads (color traces, Fig. 2B) produced much larger relative variations of sV_1 and sV_4 than short circuit and open circuit (grey and black traces Fig. 2B). In addition, important changes in phases were observed by plotting the sLEOD obtained with different capacitive loads *versus* the sLEOD obtained in the open circuit condition (color traces, Fig. 2C). This contrasts with the tight correlation between the waveforms obtained with open and short circuits (grey trace, Fig. 2C). Striking increments of the high frequency hump in the power spectral density histogram were consistently observed, becoming maximum at intermediate capacitance between 5 nF and 12.3 nF (arrow, Fig. 2D).

To analyse changes in the sLEOD waveform systematically we studied the amplitude of the different peaks as a function of object impedance. In order to compare fish of different lengths, modulation of each wave component (defined as its amplitude divided by the amplitude of the same component in the absence of object) were plotted together as a function of object longitudinal resistance (Fig. 3). For every waveform component, modulation was a sigmoidal function of object resistance (Fig. 3A–C). The load resistance value yielding a modulation equivalent to the 50% of the range was different for each wave component (68.6±8.23 kΩ; 50.72±5.23 kΩ; and 33.5±3.99 kΩ; means ± S.D., for sV_1, sV_3 and sV_4, respectively), and these differences were significant (Fischer exact test, $P<0.001$, $N=10$). Despite these differences, both the ratios sV_1/sV_3 and sV_4/sV_3 were well-fitted by monotonic functions of sV_3 with opposite slopes (red symbols, Fig. 4A,B). Thus, waveform was predictable from the total energy of the sLEOD.

For capacitive loads, ratios were not predictable from the rms value. The amplitudes of sV_1 and sV_3 increased following different sigmoidal curves (50% modulation at 20 nF for sV_1 and 8 nF for sV_3; Fischer exact test, $P<0.001$, $N=10$, Fig. 3D,E). The relative amplitude of sV_4 sharply increased with capacitance up to a maximum between 10 and 12.3 nF (Fig. 3F). Beyond this maximum the ratio sV_4/sV_3 decreased up to the short circuit value. To compare between different fish we normalised the amplitude of each wave component by the change observed between open and short circuits. The graph of sV_4/sV_3 *versus* sV_3 was fitted by an inverted U-shaped curve with its peak at approximately 8 nF (Fig. 4A, blue symbols) and the graph of sV_1/sV_3 *versus* sV3 was fitted by a U-shaped function having a minimum generated by capacitors of about 12 nF (Fig. 4B, blue symbols).

For complex impedance having both capacitive and resistive components, connected either in parallel or in series, the data points fell within the surface limited by the curves generated by pure resistive and pure capacitive loads (Fig. 4A,B). Therefore, curves generated by pure resistive and pure capacitive loads define a ‘reafferent stimulus domain’ for complex impedance cylindrical objects placed near the fovea in *G. carapo.*

A similar analysis was made in the frequency domain, because electroreceptors in pulse gymnotids have previously been classified according to their tuning curves (Bastian, 1976,

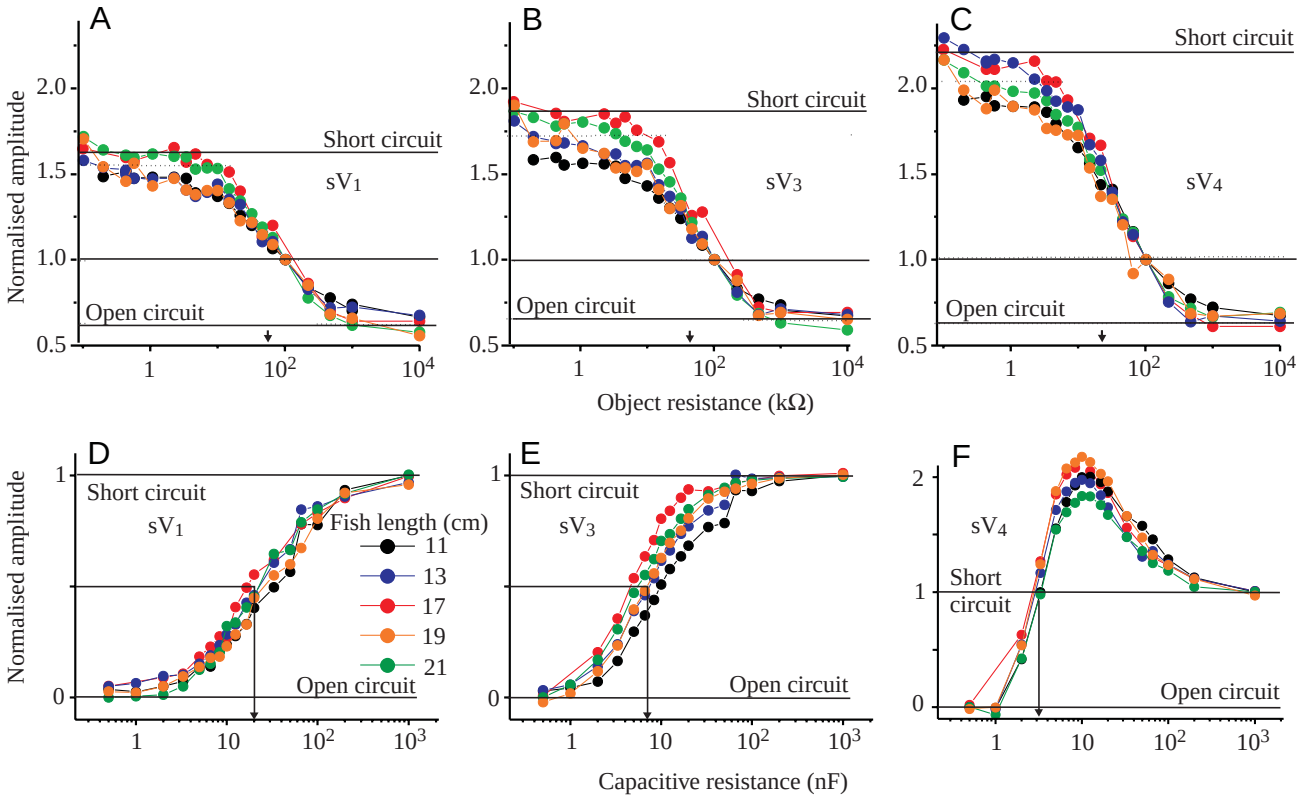

Fig. 3. Amplitude of every wave component as a function of impedance. (A–C) Resistive loads. Superimposed traces from five fish of different lengths (key in D) were normalised to their respective value in the absence of the object for each wave component. Note the differences in modulation of the different waves. Arrows indicate the resistance causing a 50% modulation of the peak of each wave component. (D–F) Capacitive loads. Superimposed traces from five fish of different lengths (key in D) were normalised to the open- and short-circuit respective values for each wave component. Note that the 50% point occurs at 20 nF for sV_1, at 7 nF for sV_3 and 2 nF for sV_4. Note also that the curve corresponding to sV_4 has a maximum at 10 nF.

1977; Yager and Hopkins, 1993). The rising flank of the spectrum (Fig. 1C) is close to the tuning frequency of low-pass burst duration coders, and the hump at the descending limb coincides with the tuning frequency of narrow band burst duration coders (Watson and Bastian, 1979). In order to evaluate the relative changes of these two zones of the spectrum, we plotted the relative power at 100 Hz and 800 Hz as a function of the total energy of the sLEOD (see below). The total energy was used because it is a good measurement of the whole spectrum stimulation potential. For resistive objects these plots show a flat profile, indicating that the signal is mainly modulated in amplitude (Fig. 5A,B, red symbols). For capacitive objects, these plots show U-shaped and inverted U-shaped profiles, respectively (Fig. 5A,B, blue symbols). These profiles are not symmetrical, indicating that there is not a 'one to one' correspondence between these parameters and that neither is redundant. Data points generated by objects having combined capacitive and resistive loads fell within the domain delimited by the lines corresponding to pure resistance and pure capacitance loads.

sLEOD amplitude and waveform discrimination

The total energy of the sLEOD (ε) can be calculated as the integral over time of the square of current density (J^2) times the specific resistance of the skin (ρ, Equation 1):

$$\varepsilon = \int J^2 \rho dt \,. \quad (1)$$

Since duration of the sLEOD is finite and constant, ε is proportional to its effective value or rms value (Cotton, 1966), defined as the direct current intensity that dissipates the same amount of energy per unit of time. Since cutaneous impedance is mainly resistive (Caputi and Budelli, 1995) and transcutaneous current density is a linear function of the sLEOD, the amplitude of the local stimulus is proportional to the total energy of the sLEOD dissipated in the adjacent water. We estimated numerically the rms value of the local stimulus as the square root of the mean of sLEOD squared values from the beginning of sV_1 to 3 ms after the peak of sV_3 (Equation 2). This last limit was arbitrarily set, due to the monotonically- and asymptotically-to-zero temporal course of sV_4:

$$\text{rms} = \sqrt{\text{mean sLEOD}^2} \,. \quad (2)$$

We found that peak amplitude of sV_3 was highly correlated

with the rms value (Fig. 6). This relationship was well fitted by the same linear function for pure resistive, pure capacitive and resistive-capacitive loads in the same fish. This result indicates that the easily measurable sV_3 was a good estimator of the total energy dissipated at the skin and consequently a good estimator of the stimulus at the center of the region facing the object. However, since electroreceptor response might be waveform-dependent, the effective stimulating energy eliciting a neural response is equivalent to the total energy attenuated by a factor, depending on receptor responsiveness to the stimulus waveform.

Using the novelty response as an index of the perceived change in an electrosensory stimulus, we explored how the amplitude of the novelty response depends on the change in stimulus energy and how changes in waveform modify this relationship. The amplitude of the novelty response caused by a change in the longitudinal resistance of a cylindrical object is not dependent on the pair of load resistors compared but on a logarithmic function of the change in the peak-to-peak amplitude of the sLEOD (a linear regression of the data in Fig. 7A yields r=0.9, N=15, P<0.0001).

Since for resistive objects the peak-to-peak amplitude is linearly related to sV_3 and to the rms value, the amplitude of the novelty response for a change in resistance alone is also a logarithmic function of the changes in sV_3 and in rms value. Linear regression analysis confirmed this hypothesis (Fig. 7A, red line; r=0.9, N=15, P<0.0001). The differences between the expected values of the amplitude of the novelty response (according to its regression *versus* sV_3) and the observed values were not significantly correlated with change either in sV_1/sV_3 or in sV_4/sV_3 (Fig. 7B,C; r=0.09 and r=0.2, respectively; N=15, P>0.4 in both cases). This lack of correlation with waveform parameters and the good correlation with the rms value suggest that the detection cue in the case of resistive objects is a function of the change in total energy of the signal.

We further tested whether this hypothesis holds for the general case of complex impedance. When the longitudinal load of the cylindrical stimulus-object was changed from

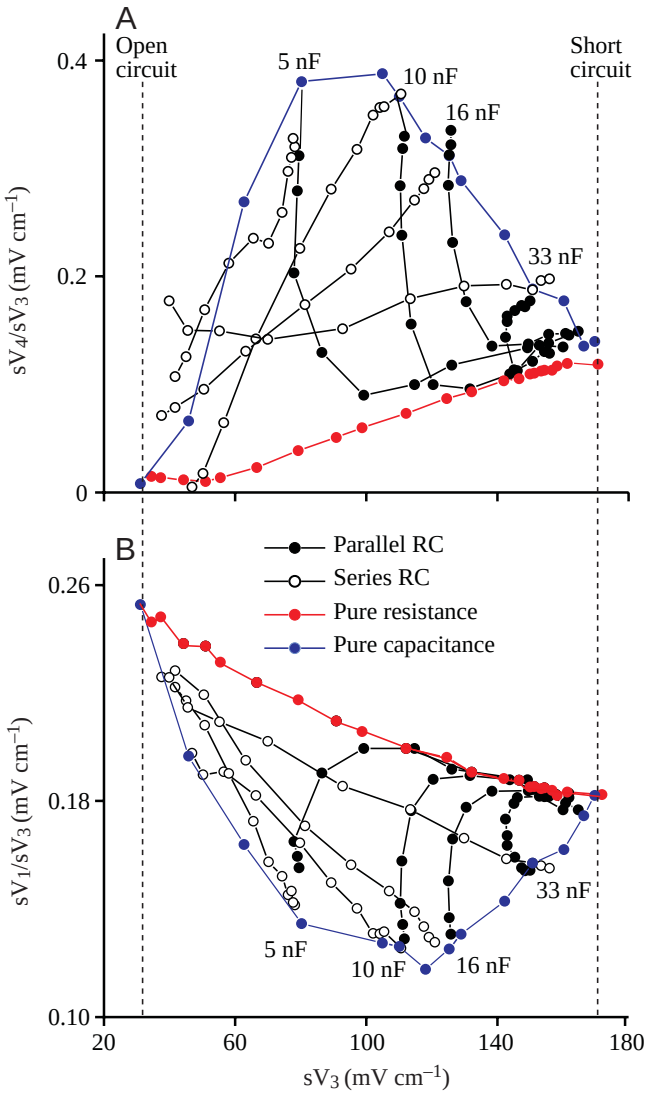

Fig. 4. Stimulus domain as defined by time-waveform parameters. (A) sV_4/sV_3 as a function of sV_3. (B) sV_1/sV_3 as a function of sV_3. Points obtained using resistive (red symbols) and capacitive (blue symbols) loads bound a domain in which are contained resistance-capacitance (RC) combinations (black filled symbols: in parallel; open symbols: in series). Note the different shape of plots A and B; for an explanation, see text.

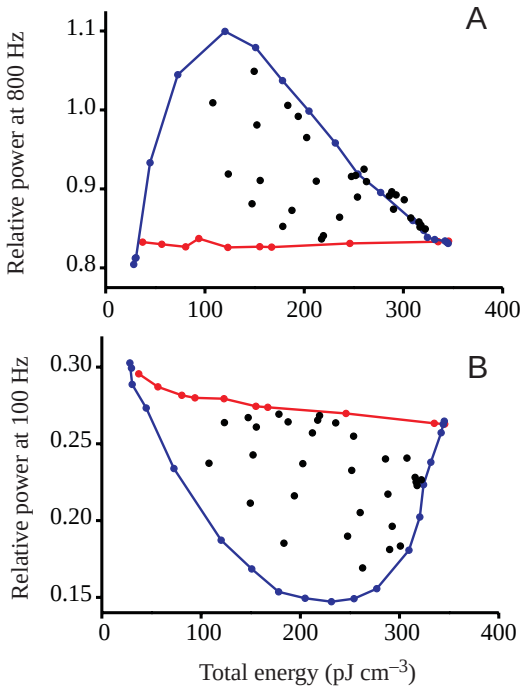

Fig. 5. Stimulus domain as defined by power spectrum parameters. (A) Relative power at the high frequency flank (where the hump occurs) as a function of rms value. (B) Relative power at the rising edge at 100 Hz as a function of rms value. Note the flat curves obtained using resistive loads (red symbols). These curves and those obtained using capacitive loads (blue symbols) bound a domain in which are contained resistance–capacitance combinations (black filled symbols: in parallel). Note the different shape of plots A and B; for an explanation, see text. Data presented in Figs 4 and 5 were obtained from different animals.

open circuit to a given capacitor (Fig. 7, blue symbols), the amplitude of the evoked novelty response was also a function of the change in sLEOD rms value. However, the function with a best fit was not monotonically increasing. Except for the very small and very large rms values, where both curves converge, the novelty responses obtained with capacitors were significantly larger than the expected value predicted by the rms change, as predicted from the experiments with resistors. Differences between this expected value and the measured amplitude of the novelty responses evoked using capacitive loads were significantly correlated with the changes in sV_1/sV_3 and in sV_4/sV_3 (Fig. 7B,C; r=0.75 in both cases, N=30, P<0.0001). Decreases in sV_1/sV_3 and increases in sV_4/sV_3 account for the difference between the observed and expected amplitudes of the novelty response. This indicated that the amplitude of the novelty response was independently correlated with both energy and waveform parameters.

To test the hypothesis that changes in waveform alone can be detected by *G. carapo*, we provoked changes in sLEOD waveform maintaining the rms value constant in five fish. Novelty responses were consistently evoked in these experiments, indicating that fish are able to detect a parameter independent of total energy. Responses were asymmetric; large novelty responses (amplitude 6–10%) were always obtained when the change in load produced a decrease of sV_1/sV_3, an increase of sV_4/sV_3 or a phase advance of the slope sV_3–sV_4. Conversely, opposite waveform changes did not modify the inter-EOD interval, or elicit changes in the inter-EOD interval that did not fulfil the typical pattern of the novelty response (small reduction of successive intervals; Fig. 8).

In order to study this phenomenon in more detail, we explored the effect of waveform changes between selected points in the above-defined stimulus domain (four points in two fish, six points in one fish). Two of these points were defined by open and short circuits (black and grey traces, respectively; Fig. 9). The other selected points were pairs of points sharing the same total energy but having different waveform parameters. In each of these pairs, one point was defined by a given capacitor and the other by the resistor generating a sLEOD of the same rms value (Fig. 9; 10 nF, blue traces and 21 kΩ, red traces). As also shown in Fig. 7, similar changes in waveform provoked novelty responses of different amplitude depending on the associated change in rms value (compare Fig.

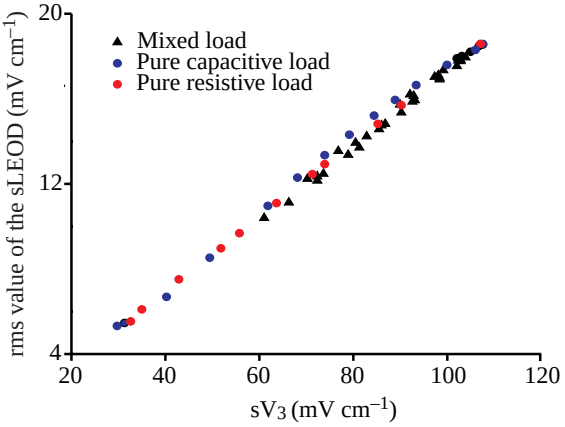

Fig. 6. Energy of the sLEOD as a function of sV_3. sLEOD rms value is a linear function of sV_3 independently of the impedance of the stimulus object. Data were obtained from the same fish with resistive loads (red symbols), capacitive loads (blue symbols) and resistive and capacitive loads connected in parallel (black symbols).

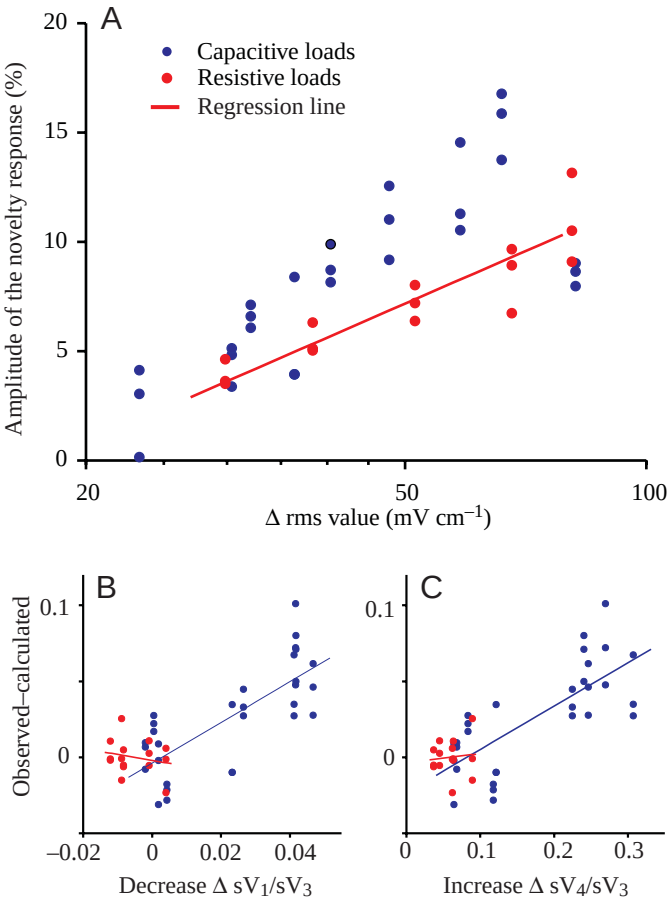

Fig. 7. Amplitude of the novelty response as a function of the change in sLEOD parameters. In these experiments, the object load was changed from open circuit to a given resistor value (red symbols) or a given capacitor value (blue symbols). (A) Amplitude of novelty response (interval shortening as a percentage of the basal interval) as a function of energy (as the change in rms value) of the sLEOD. Linear regression analysis was performed for experiments in which the change in sLEOD was obtained by loading the object with resistors: amplitude of the novelty response = 0.15×log(Δrms/0.35); r^2=0.81, N=15, P<0.0001; the regression line is drawn in red. Changes from open circuit to capacitive loads evoked larger responses than changes from open circuit to resistive loads, which generated sLEODs with the same rms value, except at the extremes of the range. (B) Difference between the predicted amplitude of the novelty response minus the measured data as a function of the $\Delta sV_1/sV_3$ ratio. The correlation was statistically significant only for experiments performed with capacitors (r^2=0.75, N=30, P<0.001). (C) Difference between the predicted amplitude of the novelty response minus the measured data as a function of the $\Delta sV_4/sV_3$ ratio. The correlation was statistically significant only for experiments performed with capacitors (r^2=0.75, N=30, P<0.001).

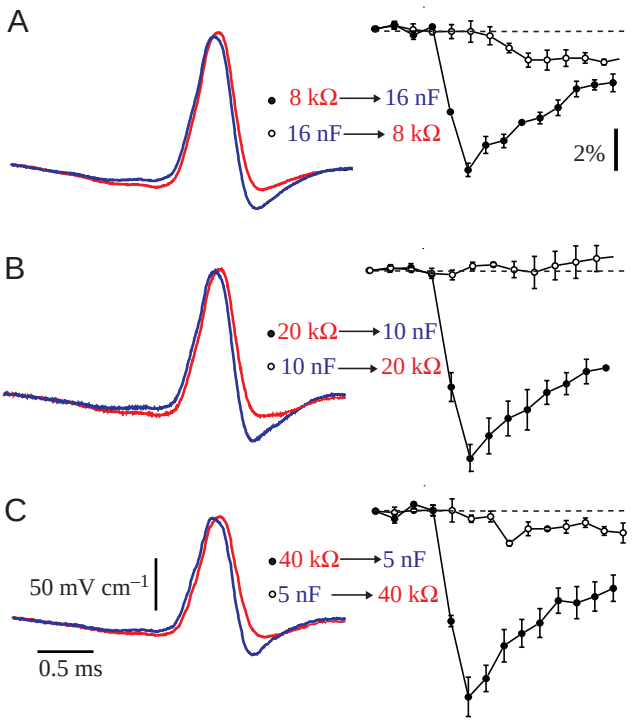

Fig. 8. Waveform changes are detected by *G. carapo*. To test if waveform changes are detected independently of changes in rms value, the load of the stimulus-object was chosen in such way that the rms values of the resulting sLEODs were the same. This was achieved by substituting a resistor (red traces) by a capacitor (blue traces) or *vice versa*. The plots on the right show that novelty responses were evoked when the impedance change was from resistance to capacitance (filled symbols) but not when the change was from capacitance to resistance (dotted line indicates the baseline interval). (A–C) Three examples from the same fish.

9B and C). Decreases of sV_1/sV_3 and/or increases of sV_4/sV_3 associated with increases in sLEOD rms value provoked novelty responses of larger amplitude than the same change in rms value associated with minimum changes in waveform (compare Fig. 9B and D). Strikingly, changes in waveform consisting of increasing sV_4/sV_3 and a phase advance of the slope sV_3–sV_4 always evoked novelty responses, even when they were associated with reduction in rms value (that otherwise did not provoke novelty responses; Fig. 9E, open symbols). On the other hand, reductions in sV_4/sV_3 did not evoke novelty responses even when they were associated with increases in rms value (that otherwise did provoke novelty responses; Fig. 9E, filled symbols). This suggests that processing of changes in waveform and total energy (estimated by the rms value) are independent and their effects on the novelty response are additive.

Discussion

Objects of size and shape similar to those of common preys modify amplitude (as measured by the rms value) and waveform (as measured by the ratios between the peaks of the sLEOD wave components) of the self-generated carrier when they were placed close to the fovea of *G. carapo*. The high density and variety of receptors in this area suggest that waveform analysis is performed in the electrosensory fovea (Castelló et al., 2000). Therefore, this region was selected to describe the significant stimulus for impedance discrimination. However, the complexity of the EOD precludes extrapolation of the results obtained at the perioral region to the rest of the body.

The analysis of the amplitude of the novelty responses provoked by the changes in sLEOD indicates that *G. carapo* discriminates resistance using a single energy-related parameter. It also discriminates complex impedance by detecting independent changes in intensity and waveform. At present we cannot assess how many independent waveform parameters are coded; nevertheless our findings, together with an analysis of findings reported in previous literature, suggest that these fish evaluate impedance-related sensory qualities of closely located objects integrating at least two parameters of the sLEOD waveform.

Modulation of the sLEOD by nearby objects

Waveform components are the sum of the fields originated in different regions of the elongated electric organ of *G. carapo* (Caputi et al., 1989, 1993; Caputi, 1999; Assad et al., 1999). The sum of effects of the series of different sources that may be used to represent the electric organ discharge depends on their relative distance to the sLEOD, on water and object impedance, and on their relative electromotive forces and internal impedance. At the electrosensory fovea, the three components of the sLEOD correspond to different sources in the EO: (i) sV_1 is generated by a low electromotive force and low internal resistance source (V_1) located at the abdominal region; (ii) sV_3 is generated all along the fish by a distributed source (V_3), increasing in electromotive force and internal resistance from head to tail; and (iii) sV_4 is generated mainly at the trunk-tail region by a source (V_4) of strong electromotive force and high internal resistance (Caputi, 1999). At the fovea, the field is large, has the same orientation all along the time course of the EOD and shows identical time waveforms all over the perioral region (Castelló et al., 2000; Aguilera et al., 2001). Due to these characteristics the modulation in sLEOD waveform caused by resistive loads is predictable from the change in total energy of the sLEOD. Nevertheless, sV_1 is less modulated than sV_3, which in turn is less modulated than sV_4, as shown in Figs 1 and 3.

When there is a capacitive load, the base of the cylinder closest to the skin is negatively charged during V_1 up to the point that the charge counterbalances the effect of the EOD-generated current; this causes a relative decay of sV_1. When the EOD current decays below this limit, opposite current flow originated in the capacitor discharge prevails and the sLEOD, resulting from the addition of both, reverses phase in advance. Thus, sV_3 begins and ends earlier than V_3. The capacitor discharges and recharges during V_3, affecting its time course: the discharge current flows in the same direction causing an advance of phase of sV_3, but the recharge current is opposed

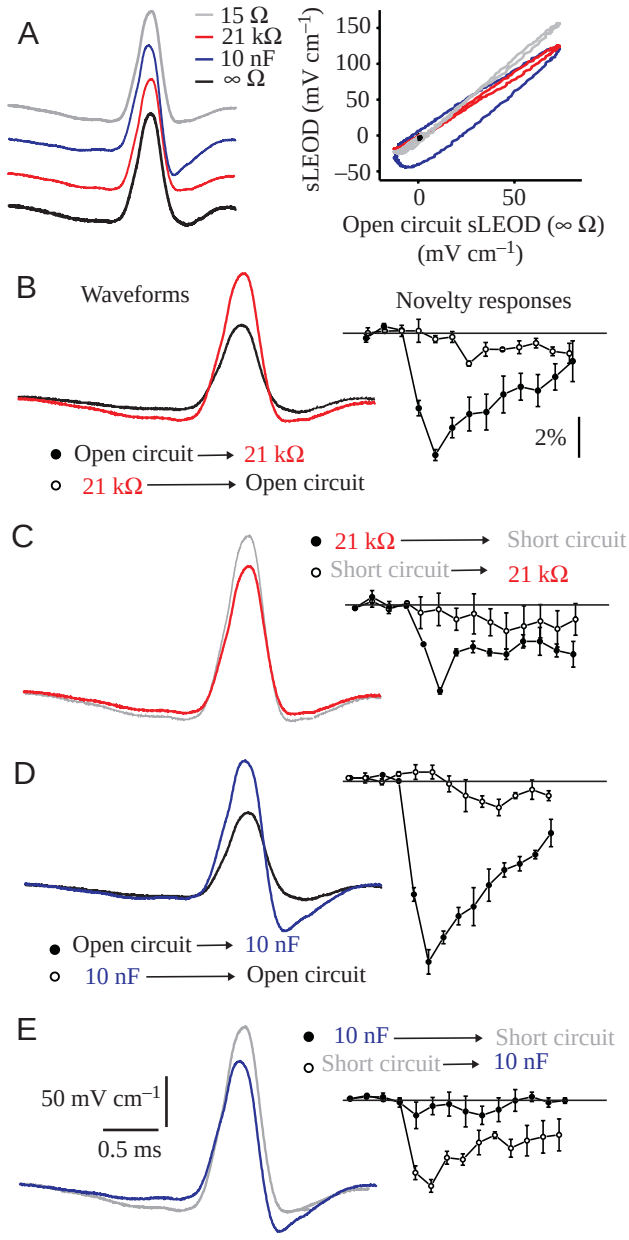

Fig. 9. Changes in waveform and amplitude have additive effects. (A) Four loads, open circuit (generating the minimum rms value, black trace), short circuit (generating the maximum rms, 15 Ω, grey trace) and two different impedances (generating the same intermediate rms value but very different waveform, a resistor of 21 kΩ, red trace, and a capacitor of 10 nF, blue trace) were selected to test whether amplitude and waveform are independently evaluated by the fish. Right: the differences in amplitude and waveform of the signals compared by the fish. The differences in amplitude are shown by the main slope of the loop and the differences in waveform by its deviation from a straight line. (B–E) Each panel represents paired experiments in which the stimulus-object impedance was changed in either direction between open circuit and resistance (B), short circuit and resistance (C), open circuit and capacitance (D) and short circuit and capacitance (E). When resistive load were used, waveform changes were small (B,C) and novelty responses were only elicited by increases in sLEOD rms value. Consistently with the experiment shown in Fig. 7, the amplitude of the elicited novelty responses was graded with the increase in rms value. When large waveform changes (caused by a capacitive load, D and E) were associated with the same changes in rms value, the amplitude of the elicited novelty responses varied as if the rms value and the waveform were independently evaluated. The amplitude of the novelty response was relatively increased by a waveform change consisting of a reduction of the early slow-negative wave plus an increase and advance of phase of the late sharp-negative wave (compare the responses marked with filled symbols in D and E). When a similar waveform change was associated with a decrease in the rms value it provoked a small novelty response (compare E, open symbols, with C, open symbols). Finally, when increases in rms value were associated with opposite changes in waveform (reduction of the late negative wave and increase of the positive-negative slope), novelty responses were not elicited (E, filled symbols)

causing the advance of phase of the following component (sV_4). Finally, currents generated at the caudal EO (V_4) summate to those driven by the capacitance discharge, enhancing sV_4.

In summary, sLEOD waveform components are the sum of effects of currents generated by the EOD and by the charge or discharge of the capacitor. The charge initially accumulated in the capacitor during V_1 (generating a virtual source opposing V_1 and thus decreasing sV_1) is delivered later. Most of this charge is finally delivered at the end of the EOD, causing an increase of sV_4. Therefore, the changes in sV_1/sV_3 and sV_4/sV_3 associated with capacitive loads are opposite.

Amplitude and waveform discrimination

The amplitude of the novelty response is scaled with the change in rms value of the reafferent signal. For resistive objects, the constancy of the shapes of the power spectra and the lack of correlation of the amplitude of the novelty response with changes in sV_1/sV_3 and sV_4/sV_3, suggest that the change in the total energy of the signal is the cue for discrimination. Correlation analyses suggest that other waveform-dependent cues are also important for complex impedance discrimination. sLEODs having different waveforms but the same rms value are clearly discriminated, indicating that a waveform-dependent parameter is used independently of sLEOD amplitude as a discrimination cue. Novelty responses were only evoked in the direction associated with decreases in sV_1/sV_3, increases in sV_4/sV_3 and phase advances in the slope sV_3–sV_4, suggesting that these parameters or their related changes in the power spectra (relative decrease in the low frequency range and increase in the high frequency range) are possible cues for waveform discrimination. Since waveform parameters were significantly correlated among themselves, we could not assess whether a single waveform parameter or a combination of parameters are sensed.

When changes in waveform were associated with increases in rms value, the provoked novelty response was much larger than when the waveform changes were associated with reductions of the rms value. This suggests that cues related to energy and waveform may have additive effects and therefore that they are probably sensed in an independent manner (see Fig. 9). In fact, previous literature indicates that pulse

gymnotids are furnished with the necessary structural features to evaluate more than a single parameter of the sLEOD (Bastian, 1976, 1977, 1986; Watson and Bastian, 1979; Yager and Hopkins, 1993). Watson and Bastian (1979) described three subtypes of burst duration coders having different frequency tuning properties. Receptor variety is particularly important in the foveal region (Castelló et al., 2000), suggesting that pulse fish evaluate a complex spectrum using different types of receptors encoding different features of the object associated signals. The similarity with color vision is clear.

Combining our data with those of Watson and Bastian (1979), we have compared the power spectral density histograms with typical tuning curves. The threshold of 'low-frequency band' receptors (best frequency below 100 Hz) follows a curve parallel to the low-frequency flank of the spectra (50% around 200 Hz), the threshold of 'narrow-band receptors' has a minimum (best frequency 500 to 2000 Hz with sharp tuning) in the frequency range where the hump occurs (between 700 and 900 Hz). The independent variation of the relative power observed at 100 Hz and 800 Hz (Fig. 8) suggests that low-frequency and narrow-band receptors code non-redundant information. Information about the total sLEOD energy may be provided by wide-band receptors (broad band tuned between 125–1000 Hz). The various frequency sensitivities allow the fish to create a multi-dimensional representation of object impedance-related stimulus features.

It should be noted that not only frequency tuning but also phase dependence has been demonstrated in electroreceptors of a related species (Heiligenberg and Altes, 1978). Pulse markers giving raise to the fast electrosensory pathway in *G. carapo* (Szabo, 1965; Castelló et al., 1998) have tuning properties similar to narrow-band burst duration coders (Watson and Bastian, 1979) and may provide phase information to integrate the signals conveyed by the three types of burst duration coders.

We thank Drs M. Castelló and O. Trujillo-Cenóz for their valuable comments. This work was partially supported by Fogarty Grant no. 1R03·-TW05680-01 and PEDECIBA (doctorate fellowship to P.A.).

References

Aguilera, P. A., Castelló, M. E. and Caputi, A. A. (2001). Electroreception in *Gymnotus carapo*: differences between self-generated and conspecific-generated signal carriers. *J. Exp. Biol.* **204**, 185-198.

Assad, C., Rasnow, B. and Stoddard, P. K. (1999). Electric organ discharges and electric images during electrolocation. *J. Exp. Biol.* **202**, 1185-1193.

Bastian, J. (1976). Frequency response characteristics of electroreceptors in weakly electric fish (Gymnotidei) with a pulse discharge. *J. Comp. Physiol. A* **112**, 165-180.

Bastian, J. (1977). Variations in the frequency response of electroreceptors dependent on receptors location in weakly electric fish (Gymnotidei) with a pulse discharge. *J. Comp. Physiol. A* **121**, 53-64.

Bastian, J. (1986). Electrolocation: Behavior, Anatomy, and Physiology. In *Electroreception* (ed. T. H. Bullock and W. Heiligenberg), pp. 577-612. New York: Wiley.

Bell, C. C. (1990). Mormyromast electroreceptor organs and their afferent fibers in mormyrid fish. III. Physiological differences between two morphological types of fibers. *J. Neurophysiol.* **63**, 319-332.

Budelli, R. and Caputi, A. A. (2000). The electric image in weakly electric fish. Perception of objects of complex impedance. *J. Exp. Biol.* **203**, 481-492.

Bullock, T. H. (1969). Species differences in effect on electroreceptor input on electric organ pacemakers and other aspects of behaviour in electric fish. *Brain Behav. Evol.* **2**, 85-118.

Caputi, A. A. (1999). The EOD of pulse gymnotiforms, from a single impulse to a complex electromotor pattern. *J. Exp. Biol.* **202**, 1229-1241.

Caputi, A. and Budelli, R. (1995). The electric image in weakly electric fish: I. A data-based model of waveform generation in *Gymnotus carapo*. *J. Comput. Neurosci.* **2**, 131-147.

Caputi, A., Macadar, O. and Trujillo-Cenóz, O. (1989). Waveform generation in *Gymnotus carapo*. III. Analysis of the fish body as an electric source. *J. Comp. Physiol. A* **165**, 361-370.

Caputi, A., Silva, A. and Macadar, O. (1993). Electric organ activation in *Gymnotus carapo:* spinal and peripheral mechanisms. *J. Comp. Physiol. A* **173**, 227-232.

Castelló, M. E., Aguilera, P. A., Trujillo-Cenóz, O. and Caputi, A. A. (2000). Electroreception in *Gymnotus carapo*: pre-receptor processing and the distribution of electroreceptor types. *J. Exp. Biol.* **203**, 3279-3287.

Castelló, M. E., Caputi, A. A. and Trujillo-Cenóz, O. (1998). Structural and functional aspects of the fast electrosensory pathway in the electrosensory lateral line lobe of the pulse fish *Gymnotus carapo*. *J. Comp. Neurol.* **401**, 549-563.

Cotton, H. (1966). *Principles of Electrical Technology*. London: Sir Isaac Pitman and Sons Ltd.

Dye, J. C. and Meyer, J. H. (1986). Central control of the electric organ discharge in weakly electric fish. In *Electroreception* (ed. T. H. Bullock and W. Heiligenberg), pp. 577-612. New York: Wiley.

Heiligenberg, W. (1991). *Neural Nets in Electric Fish.* Cambridge: London MIT Press.

Heiligenberg, W. and Altes, R. (1978). Phase sensitivity in electroreception. *Science* **199**, 1001-1004.

Hopkins, C. D. (1976). Stimulus filtering and electroreception: tuberous electroreceptors in three species of gymnotoid fish. *J. Comp. Physiol. A* **111**, 171-200.

Hopkins, C. D. (1983). Functions and mechanisms in electroreception. In *Fish Neurobiology* (ed. R. G. Northcutt and R. E. Davis), pp. 215-259. Ann Arbor: University of Michigan Press.

Lissmann, H. W. (1951). Continuous electrical signals from the tail of a fish, *Gymnarchus niloticus* Cuv. *Nature* **167**, 201-202.

Lissmann, H. W. (1958). On the function and evolution of electric organs in fish. *J. Exp. Biol.* **35**, 156-191.

Lissmann, H. W. and Machin, K. E. (1958). The mechanism of object location in *Gymnarchus niloticus* and similar fish. *J. Exp. Biol.* **35**, 451-486.

Meyer, J. H. (1982). Behavioral responses of weakly electric fish to complex impedances. *J. Comp. Physiol. A* **145**, 459-470.

Moller, P. (1995). *Electric Fishes. History and Behavior*. London: Chapman and Hall.

Scheich, H., Bullock, T. H. and Hamstra, R. H. (1973). Coding properties of two classes of afferent nerve fibers: High frequency electroreceptors in the electric fish *Eigenmannia*. *J. Neurophysiol.* **36**, 39-60.

Sicardi, A. E., Caputi, A. A. and Budelli, R. (2000). Physical basis of electroreception, *Physica A* **283**, 86-93.

Szabo, T. (1967). Activity of peripheral and central neurons involved in electroreception. In *Lateral Line Detectors* (ed. P. Cahn), pp. 295-311. Bloomington: Indiana University Press.

Szabo, T. and Fessard, A. (1965). Le functionnement des électrorrècepteurs étudié ches les Mormyres. *J. Physiol. Paris* **57**, 343-360.

von der Emde, G. (1990). Discrimination of objects through electrolocation in the weakly electric fish *Gnathonemus petersii*. *J. Comp Physiol. A* **167**, 413-421.

von der Emde, G. (1993). The sensing of electric capacitances by weakly electric mormyrid fish: effects of water conductivity. *J. Exp. Biol.* **181**, 157-173.

von der Emde, G. (1999). Active electrolocation of objects in weakly electric fish. *J. Exp. Biol.* **202**, 1205–1215.

von der Emde, G. and Bell, C. (1994). Responses of cells in the mormyrid electrosensory lobe to EODs with distorted waveforms: implications for capacitance detection. *J. Comp. Physiol. A* **175**, 83-93.

von der Emde, G. and Ronacher, B. (1994). Perception of electric properties of objects in electrolocating weakly electric fish: Two-dimensional similarity scaling reveals a City-Block-Metric. *J. Comp. Physiol. A* **175**, 801-812.

von der Emde, G. and Bleckmann, H. (1997). Waveform tuning of electroreceptor cells in weakly electric fish *Gnathonemus petersii*. *J. Comp. Physiol. A* **181**, 511-524.

Watson, D. and Bastian, J. (1979). Frequency response characteristics of electroreceptors in the weakly electric fish *Gymnotus carapo*. *J. Comp. Physiol. A* **134**, 191-202.

Werner, G. (1980). The study of sensation in physiology: psychophysical and neurophysiological correlations. In *Medical Physiology* (ed. V. B. Mountcastle), pp. 605-628. St Louis: The C.V. Mosby Company.

Yager, D. D. and Hopkins, C. D. (1993). Directional characteristics of tuberous electrorreceptors in the weakly electric fish *Hypopomus* (Gymnotiformes). *J. Comp. Physiol. A* **143**, 401-414.